

## Article

# Predicting Dynamic Coastal Delta Change in Response to Sea-Level Rise

Wietse I. Van De Lageweg <sup>1,\*</sup> and Aimée B. A. Slangen <sup>2</sup><sup>1</sup> Geography and Geology, School of Environmental Sciences, University of Hull, Hull 7RX, UK<sup>2</sup> Royal Netherlands Institute for Sea Research (NIOZ), Department of Estuarine and Delta Systems (EDS), Utrecht University, Yerseke 4400 AC, The Netherlands; aimee.slangen@nioz.nl

\* Correspondence: wietse.vandelageweg@gmail.com; Tel.: +31-113-577-300

Received: 9 May 2017; Accepted: 16 June 2017; Published: 20 June 2017

**Abstract:** The world's largest deltas are densely populated, of significant economic importance and among the most valuable coastal ecosystems. Projected twenty-first century sea-level rise (SLR) poses a threat to these low-lying coastal environments with inhabitants, resources and ecology becoming increasingly vulnerable to flooding. Large spatial differences exist in the parameters shaping the world's deltas with respect to river discharge, tides and waves, substrate and sediment cohesion, sea-level rise, and human engineering. Here, we use a numerical flow and transport model to: (1) quantify the capability of different types of deltas to dynamically respond to SLR; and (2) evaluate the resultant coastal impact by assessing delta flooding, shoreline recession and coastal habitat changes. We show three different delta forcing experiments representative of many natural deltas: (1) river flow only; (2) river flow and waves; and (3) river flow and tides. We find that delta submergence, shoreline recession and changes in habitat are not dependent on the applied combination of river flow, waves and tides but are rather controlled by SLR. This implies that regional differences in SLR determine delta coastal impacts globally, potentially mitigated by sediment composition and ecosystem buffering. This process-based approach of modelling future deltaic change provides the first set of quantitative predictions of dynamic morphologic change for inclusion in Climate and Earth System Models while also informing local management of deltaic areas across the globe.

**Keywords:** sea level; delta; numerical modelling; tides; waves; coastal erosion; coastal flooding; coastal habitat; coastal management

## 1. Introduction

Future impacts from sea-level rise (SLR) are expected to be widespread in low-lying deltaic coastal areas [1–3]. River-dominated deltas such as the Mississippi delta have a different morphology compared to wave-influenced deltas such as the Nile delta and tide-influenced deltas such as the Ganges delta, reflecting primarily the interplay between the sediment input by rivers [4] and the marine reworking of these sediments by tides and wave action [5,6]. In addition to these global differences in river input, tides and waves, regional patterns in SLR exist [7] that can deviate substantially from the global mean [8]. A key question is whether the differences in these parameters controlling delta dynamics and evolution affect the ability of deltas to respond to SLR, and hence the impact SLR has on the different delta coasts. Such an assessment taking into account global differences in river input, tides and waves and regional patterns in SLR would allow us to develop coastal impact estimates tailored to local conditions rather than global mean values.

Coastal environments provide a range of ecosystem services for many endangered species [9]. Despite observations that coastal wetlands in the intertidal zone can persist for thousands of years [10], more recent studies indicate increased submergence of marshes due to SLR [1,11], resulting in

a conversion from diverse marsh ecosystems to unvegetated subtidal habitats. Understanding and predicting such coastal response developments, their rates of change and the identification of vulnerable and resilient coastal environments is vitally important to informing future flood management and the sustainable planning of coastal habitats.

Deltaic coasts can either respond dynamically to SLR, potentially mitigating the effect of SLR, or they can be inundated [12]. Inundation assessments assume a static coastal topography which is flooded to the highest level to which the water rises (i.e., “bathtub” approach) [13]. Such assessments fail to include the dynamic response due to hydrodynamic [5], ecological [11] and morphological [14] processes such as erosion and deposition that shape deltaic coasts. The dynamic response potential for many coastal environments is quantitatively uncertain, yet crucially important to understanding how the projected SLR will be translated into coastal impact. Flooding risk and coastal erosion will increase due to the higher water levels resulting from SLR [14,15], particularly along developed coasts with fixed coastal engineering solutions [16] and low-elevation infrastructure and housing with limited capacity to respond dynamically.

Here, we conduct morphodynamic simulations using the morphodynamic model Delft3D [4,17] to systematically evaluate the dynamic response of deltas to SLR. Specifically, we aim to: (1) quantify the capability of different types of deltas (i.e., river deltas, river- and wave-influenced deltas, and river- and tide-influenced deltas) to dynamically respond to SLR; and to (2) evaluate the resultant coastal impact by assessing delta flooding, shoreline recession and coastal habitat changes. The modelling approach is generic, with boundary conditions representative for many natural deltaic systems yielding quantitative predictions for the landward translation of dynamic deltaic shorelines.

## 2. Materials and Methods

The numerical model Delft3D (v. 5.00.10.1983) simulates flow, sediment transport and morphologic change across a range of spatial and temporal scales in coastal and fluvial environments [4,17,18]. We conduct morphodynamic simulations by varying the type of deltaic coastal forcing (three types) and the rate of SLR (four scenarios) while holding all other factors constant. These twelve simulations of delta morphodynamics are conducted with a river discharge of 1000 m<sup>3</sup>/s, carrying equilibrium sandy sediment concentrations into an ocean basin [4] (Table 1).

The ocean basin is forced linearly with twenty-first century projected sea-level rise scenarios from the Intergovernmental Panel on Climate Change Fifth Assessment Report, [3] (IPCC AR5): 0 cm (control run), 26 cm (lower bound of the Representative Concentration Pathway (RCP)2.6 scenario [19]), 47 cm (mean of the RCP4.5 scenario) and 82 cm (upper bound of the RCP8.5 scenario). By using a wide range of values we implicitly study the effect of spatially-variable SLR, with higher SLR projected in equatorial regions and lower SLR towards the poles [7,8].

**Table 1.** Model parameters and descriptive statistics of delta coasts for modeling experiments used in this study. All scenarios use a constant river discharge of 1000 m<sup>3</sup>/s. Observations (“obs”) of shoreline retreat are computed from 19 shore profiles across the modelled deltas, predictions (“pred”) are based on the Bruun (1988) [20] rule applied to the same 19 shore profiles for each modelled delta. Comparisons show a smaller ability to dynamically adjust when using a different sediment transport formulation (R\_82\_EH), but a greater ability when using finer sediment (R\_82\_FI). SLR: sea-level rise. TR: tidal range. H<sub>sig</sub>: significant wave height. St. Dev.: standard deviation. R\_82\_EH: sensitivity analysis in which the Engelund-Hansen sediment transport formulation is used rather than the Van Rijn formulation. R\_82\_FI: sensitivity analysis in which a finer sediment of 100 µm was used rather than the 225 µm sand in the main runs.

Run ID	Delta Forcing			Delta Submerged Area (d) = Dynamic Response, (s) = Static Response				Average ± St. Dev. Shoreline Retreat	
	SLR (cm)	TR (m)	H <sub>sig</sub> (m)	% <0 m MSL	% <+0.26 m MSL	% <+0.47 m MSL	% <+0.82 m MSL	Obs. (m)	Pred. (m)
<b>River Only</b>									
R_0	0	0	0	48 (d)	71 (s)	84 (s)	96 (s)	-	-
R_26	26	0	0	-	55 (d)	73 (s)	92 (s)	314 ± 454	135 ± 31
R_47	47	0	0	-	-	64 (d)	90 (s)	445 ± 262	243 ± 56
R_82	82	0	0	-	-	-	70 (d)	666 ± 320	425 ± 97
<b>River and Tide</b>									
RT_0	0	1.5	0	59 (d)	74 (s)	85 (s)	98 (s)	-	-
RT_26	26	1.5	0	-	67 (d)	78 (s)	93 (s)	234 ± 479	153 ± 45
RT_47	47	1.5	0	-	-	74 (d)	89 9s)	491 ± 417	276 ± 81
RT_82	82	1.5	0	-	-	-	81 (d)	843 ± 375	481 ± 140
<b>River and Wave</b>									
RW_0	0	0	0.5	59 (d)	79 (s)	89 (s)	98 (s)	-	-
RW_26	26	0	0.5	-	68 (d)	82 (s)	97 (s)	213 ± 254	160 ± 30
RW_47	47	0	0.5	-	-	72 (d)	94 (s)	371 ± 349	290 ± 54
RW_82	82	0	0.5	-	-	-	83 (d)	821 ± 280	505 ± 96
<b>Sensitivity tests</b>									
R_82_EH	82	0	0	-	-	-	76 (d)	-	-
R_82_FI	82	0	0	-	-	-	67 (d)	-	-

To explore the coastal impact for a range of deltaic environments, the SLR projections are combined with three types of deltaic coastal forcing: (1) a river-only experiment; (2) an experiment where tides with an amplitude of 0.75 m are included; and (3) an experiment where waves with a significant height of 0.5 m are applied.

The control run consists of a river continually discharging 1000 m<sup>3</sup>/s of water with equilibrium sediment concentrations into a standing body of water, thus forming a river delta. In the tidally-influenced runs, micro-tidal forcing with a tidal range of 1.5 m is applied at the ocean boundary, and the delta is exposed to simplified tides with a sinusoidal shape. To evaluate wave-influenced deltas, the morphologic module of Delft3D is coupled to a standalone wave module (SWAN, Simulating Waves Nearshore) [21]. The wave module simulates waves nearshore with the significant wave height set to 0.5 m, a set peak period of 5 s and otherwise default parameters.

We use an ocean basin of 300 by 225 grid cells, every 25 m<sup>2</sup>, which is identical to the model setup in Edmonds & Slingerland (2010) [4]. In agreement with their setup, initial basin depths range from 1 m to 3.5 m and white noise with a mean of 0 m and a standard deviation of 0.05 m is added to the initial bathymetry to mimic natural variations. Bed roughness is assumed constant in space and time and set to a Chezy value of 45 m<sup>0.5</sup>/s. A uniform sand-sized sediment of 225 µm, representative of many deltaic coastal environments, is used and the Van Rijn [22,23] parameterization is selected to calculate sediment transport. A sensitivity analysis evaluating the effects of the applied sediment transport formulation (i.e., Van Rijn and the Engelund–Hansen [24] formulations) and sediment size is included and will be discussed in Section 3.2. In all experiments an initial 2.5-m-thick layer of sediment is available for erosion of the bed.

The coastal deltas are forced linearly with IPCC projected global mean sea-level rise of 0 cm (i.e., no SLR), 26 cm, 47 cm and 82 cm over a century [3], thus simulating delta dynamics as a function of projected sea level from today until approximately 100 years ahead. A modelling time step of six seconds is selected to satisfy the Courant criterion. As successfully applied in other model studies [18], one model day is assumed to represent the integrated morphologic effects of a year of river flow, a year of tidal action, or a year of wave action in nature. Therefore, 100 days of delta morphological evolution are simulated while applying a morphologic factor of 25 to scale up the rate of morphologic change and the delta volume and land area [25].

We quantify the dynamic delta response and resultant coastal impact by evaluating delta flooding, shoreline recession, and bed level changes, resulting in coastal habitat alteration for the three delta types forced by the four SLR scenarios. Therefore, delta statistics are calculated to quantitatively summarize and compare the different scenarios. Characterization of the delta morphology and shoreline is done using mathematical morphological operators [26] using default MATLAB commands. Delta land area is calculated by selecting all cells above mean sea level multiplied by the cell area. The number of bifurcations in the delta is determined by applying the MATLAB *bwmorph* morphologic process “thin” on channels actively transporting sediment to end up with a skeleton from which the number of nodes is observed. The number of channels at the shoreline (“endpoints”) is calculated following a similar morphologic procedure selecting the channel skeleton endpoints. Shoreline sinuosity is calculated as a measure of shoreline rugosity with a higher sinuosity corresponding to a more rugose shoreline.

### 3. Results

#### 3.1. Delta Morphodynamics

In each simulation, a self-formed delta with a distributary channel network is generated (Figure 1). Formation of the modelled deltas proceeds from the same processes as observed in the field [27] and physical [28] and numerical [4] modelling of low-cohesion deltas. Initially, a turbulent plume aggrades and develops subaqueous levees and a subaqueous bar seaward of the river. The subaqueous bar then stagnates, causing an unstable channel bifurcation which generally results in the closure of one arm. Continued progradation and aggradation eventually leads to subaerial bifurcations, where water and sediment are distributed across large parts of the delta topset by frequent crevasse splays breaking through the thin and easily erodible levees (see Supplementary Movies detailing the morphodynamic evolution for all twelve runs).

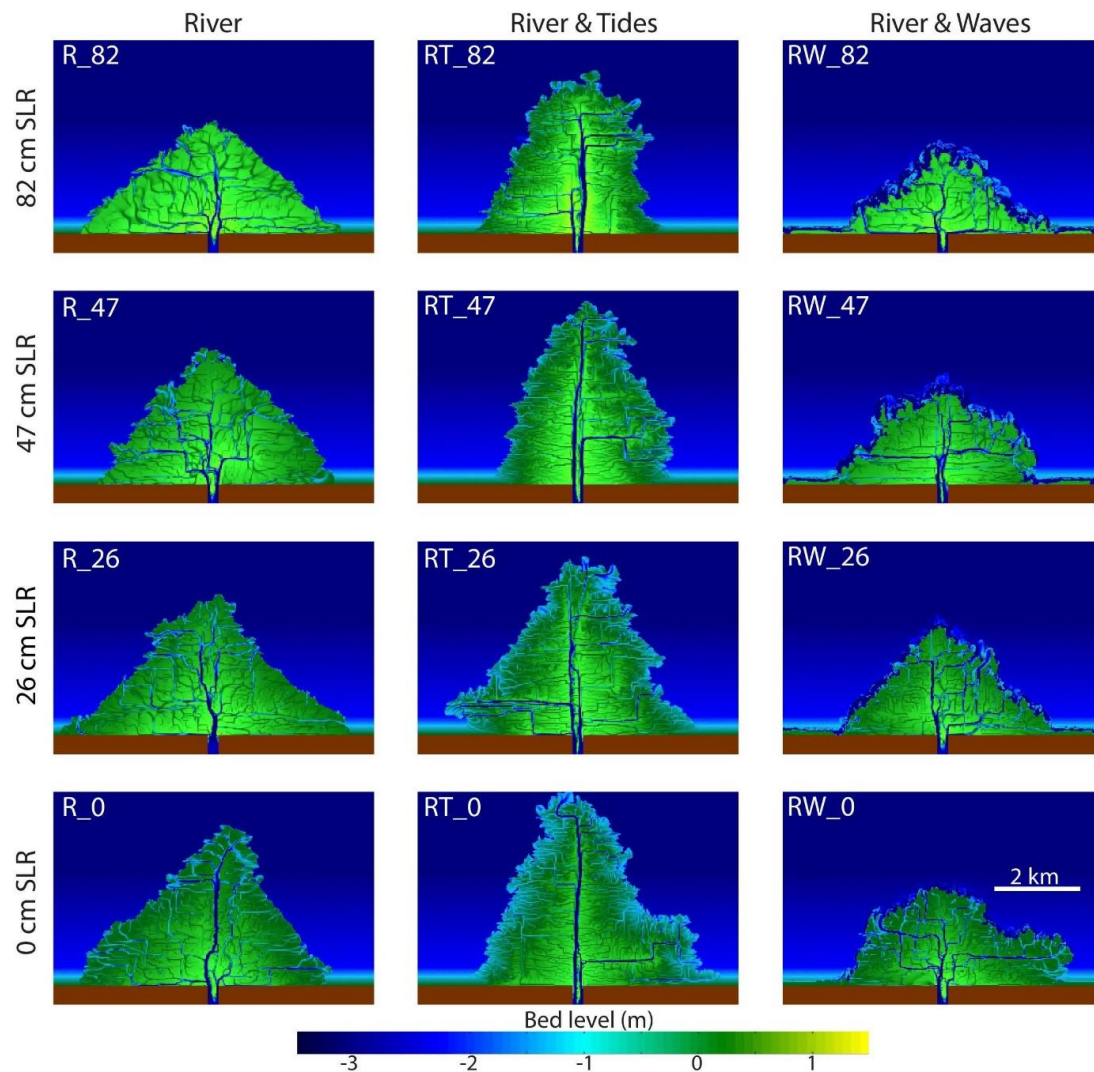


**Figure 1.** Deltaic bed levels (m) after 100 model-days, approximately corresponding to 100 years of natural evolution. Delta coast morphology as a function of coastal forcing (**left**: river discharge, **middle**: tides, **right**: waves) and sea-level scenario (from 82 cm at the top row to 0 cm at the bottom row). Animated videos of all scenarios showing delta dynamics over time are available as Supplementary Files.

The modelled deltas are compared after allowing sediment transport, deposition and hydrodynamic reworking for a century, which is the time scale of the SLR projections. Differences in the final sediment volume between the river-dominated, tidally-influenced and wave-influenced deltas, even in the absence of SLR (Figure 1, bottom row), are explained by the higher sediment-carrying competence of the river for higher seaward flow velocities in the river-only delta and during the ebb stages in the tidally-influenced delta.

The modelled deltas share many similarities with observations of natural deltas such as: (1) a wetted delta area of approximately 50% in the absence of SLR (Table 1), comparable to wet/dry ratios measured in the field [29]; (2) an increase in shoreline rugosity for tidally-influenced deltas and a decrease in shoreline rugosity for wave-influenced deltas, in agreement with natural deltas [5,26] (Table 2); and (3) the number of mouth bar channels at the shoreline decreases as a function of SLR (Table 2), consistent with observations from Holocene deltas [30].

**Table 2.** Auxiliary descriptive statistics of delta coasts for modeling experiments used in this study.

Run ID	Subaerial Area (km <sup>2</sup> )	Number of Bifurcations	Number of Channel Endpoints	Shoreline Sinuosity (-)	Minimum Elevation (m)	Median Elevation (m)	Maximum Elevation (m)
R_0	14.6	48	55	1.91	−5.92	0.02	1.25
R_26	13.5	57	39	1.54	−5.26	0.22	1.54
R_47	12.7	65	36	1.77	−5.53	0.35	1.36
R_82	11.1	33	36	1.55	−5.05	0.66	1.51
RT_0	17.2	37	50	1.97	−6.02	−0.17	1.25
RT_26	16.0	55	53	1.96	−5.15	−0.06	1.35
RT_47	14.4	28	35	1.96	−5.76	0.05	1.41
RT_82	13.0	36	32	1.84	−5.44	0.26	1.66
RW_0	12.5	69	21	1.76	−5.36	−0.08	1.29
RW_26	11.7	56	32	1.68	−5.50	0.01	1.35
RW_47	11.9	37	26	1.60	−5.45	0.01	1.31
RW_82	9.6	45	28	1.60	−5.30	−0.82	1.46
R_82_EH	-	-	-	-	−5.05	−0.03	2.40
R_82_FI	-	-	-	-	−5.26	0.71	1.54

### 3.2. Dynamic Delta Response to SLR

A key outcome of the numerical simulations is that the dynamic response to SLR is similar for the different types of modelled deltas, independent of the delta forcing (Table 1). For the highest SLR scenario of 82 cm, the modelled deltas show a land loss of 22% for river-dominated, tidally-influenced and wave-influenced deltas. Such dramatic flooding and loss of delta area for 82 cm of SLR highlight the low gradients and the lack of substantial topography on the modelled deltas, which is in agreement with many natural deltas [31]. For the lower SLR scenarios of 26 cm and 47 cm and allowing for a dynamic coastal response, the loss of delta area is smaller and amounts to 8% and 15%, respectively (Table 1).

The implication of these findings is that the regional patterns in SLR will largely determine the coastal impact in deltaic environments, irrespective of whether the delta is shaped primarily by river input, tides or waves. This means that the projected spatial patterns in SLR [7,8] can be used as a proxy for delta coastal impact globally. For example, the Amazon delta in Brazil is located in a region with a higher-than-global-mean SLR and coastal impacts are therefore expected to be more severe, while the Ganges delta in India and Bangladesh is located in a region with a lower-than-global-mean SLR and coastal impacts of climate-change driven SLR are therefore expected to be less severe. It is, however, important to note that the aforementioned coastal impacts are only related to SLR and not to land subsidence [32,33], which is substantial in the Ganges delta region and will be discussed in more detail in Section 4. Despite being shaped by different degrees of fluvial input and marine reworking, our results indicate a similar ability to dynamically respond to SLR for the aforementioned deltas thus rendering them unable to mitigate the regional differences in SLR.

Simulations performed with a finer sediment of 100  $\mu\text{m}$  indicate a higher capacity of deltaic coasts to dynamically respond to SLR (Table 1, RH\_82\_FI). The suspended sediment fraction increases for finer-grained sediment allowing for more efficient delta aggradation to dynamically respond to SLR. This, in turn, indicates an increased resilience to coastal flooding due to SLR for finer-grained suspension-dominated delta systems compared to coarser-grained bedload-dominated deltas. Additional sensitivity tests in which we changed the sediment transport calculation from Van Rijn [22,23] to the Engelund–Hansen formulation [24] show changes in the depth of channels and the elevation of bars but the overall delta morphology and the ability to dynamically respond to SLR are similar (Table 1, RH\_82\_EH).



By allowing dynamic adjustment, delta coasts maintain an additional 11%, 19% and 20% of surface area emerged compared to static coasts with SLRs of 26 cm, 47 cm and 82 cm, respectively, due to morphological processes and adaptation (Table 1). The difference between a SLR of 47 cm and a SLR of 82 cm is small and indicative of the limits of delta coasts to dynamically adjust by morphological processes to these higher SLR rates. The over-prediction of land submergence by static inundation models is consistent with natural coastal systems [12]. These findings highlight the inability of static model approaches to correctly predict the flooding impact of future deltas.

In addition to the flooding of land due to SLR, the modelled deltas show a shift in the bed level distribution, affecting coastal habitat distribution (Figure 2). Particularly relevant are marshes situated on coastal platforms in the intertidal range for which minor changes in topography and hydrodynamics can lead to vegetation disturbance and thus cause rapid marsh degradation [34]. The general deepening of the delta relative to mean sea level and the gentler slope of the coastal platform in the modelled deltas for higher SLR along with a change in flow velocity range (Figure 3) may well have significant implications for coastal marsh survival. Our simulations indicate an increase of 17% (Figure 3B) and 23% (Figure 3C) of the coastal platform submerging to subtidal levels and below the wave base, respectively, representing an important threshold below which the coastal platform cannot sustain vegetation growth [11,35]. Essentially, SLR causes parts of the intertidal area to be replaced by subtidal area, limiting the diversity of coastal habitats and suitability for many coastal species.

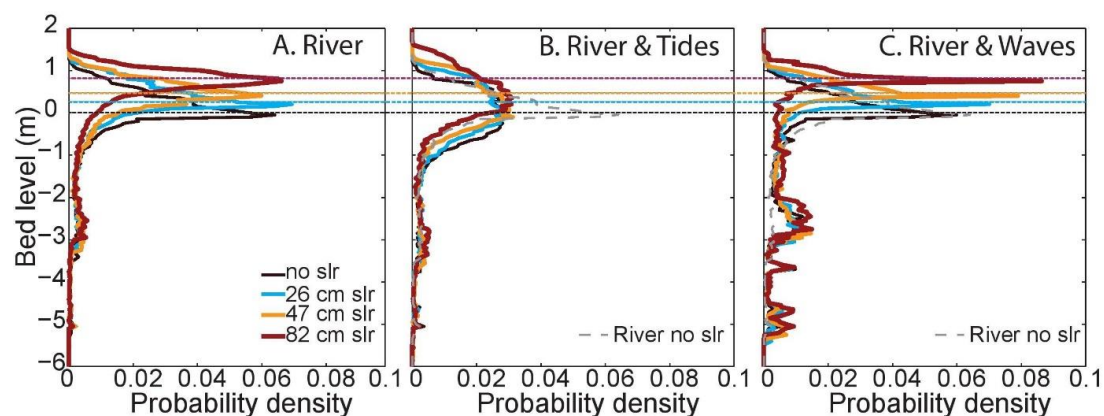


**Figure 2.** Delta bed level (m) as a function of sea-level rise scenario and coastal forcing. (A) River-dominated coasts; (B) River- and tidally-influenced coasts; (C) River- and wave-influenced coasts. Projected sea levels in 2100 indicated by horizontal lines.

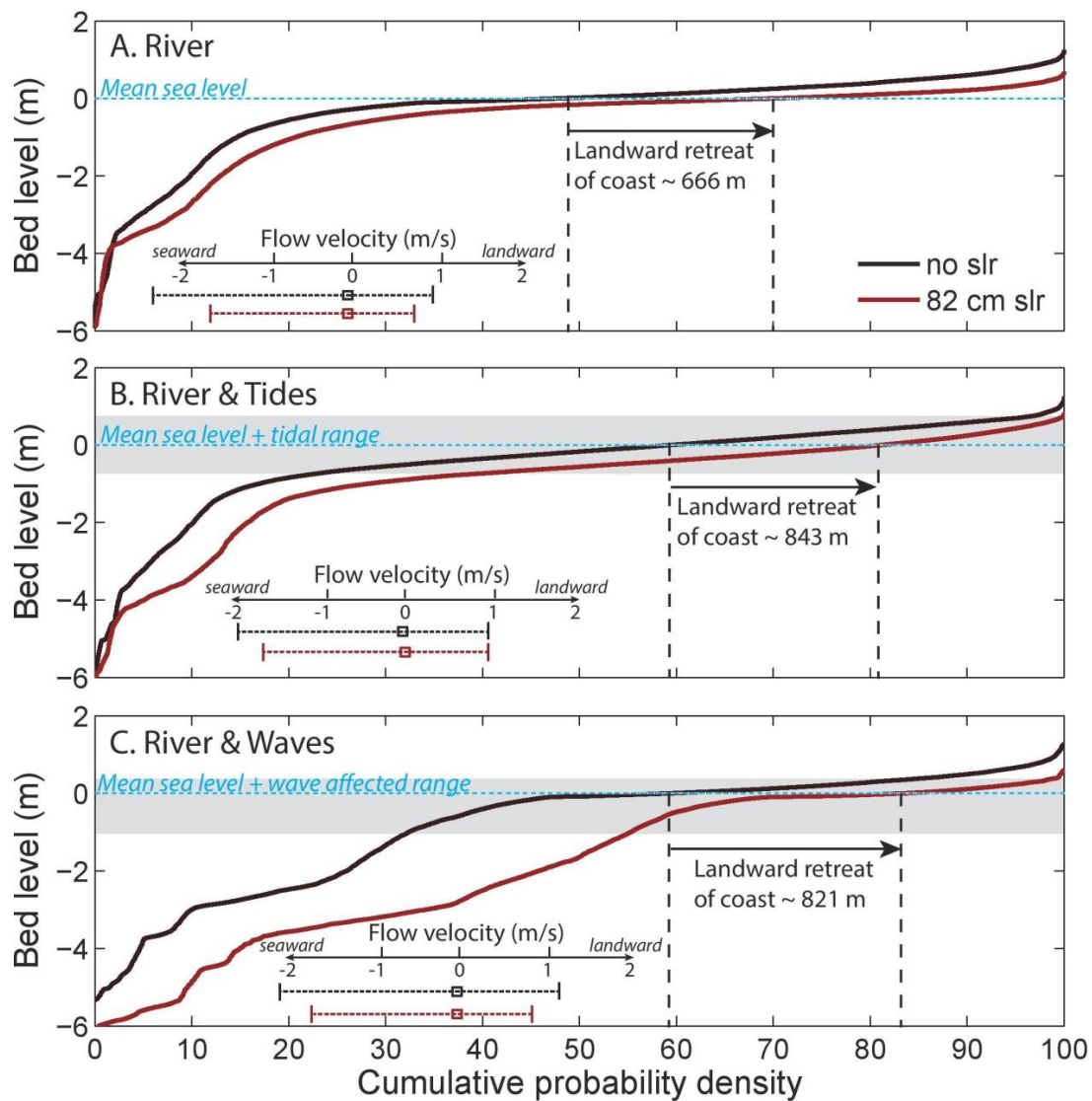


**Figure 3.** Integrated shoreline profiles relative to the mean sea level for deltas with SLRs of 0 cm (black) and 82 cm (red). (A) River-dominated delta coasts; (B) River- and tidally-influenced delta coasts. The simulated tidal range of 1.5 m is indicated in grey; (C) River- and wave-influenced delta coasts. The simulated wave range is indicated in grey with an upper range of 0.5 m, corresponding to the simulated significant wave height. The lower bound corresponds to the wave base, which is calculated as 0.5 times the wave length (in turn, calculated as wave velocity (0.5 m/s) times wave period (5 s)). The transition from subaqueous to subaerial delta is indicated by the horizontal blue dash line (see also Table 1 for descriptive statistics). The difference between the vertical black dash lines corresponds to the average shoreline retreat between 0 cm and 82 cm of SLR. Flow velocity statistics show a decreased velocity range for deltas with 82 cm SLR compared to no SLR.

### 3.3. Coastal Recession

SLR also drives coastal recession (Figure 3), potentially threatening natural and built environments of high economic and societal value [9,12,14]. The modelled deltas show a coastal recession of up to about 1 km over a 100-year period, equating to 10 meters per year, for an 82-cm SLR (Table 1). It is important to note that coastal recession is highly variable along the modelled deltaic coasts with some parts of the delta coast remaining fixed in position or even advancing slightly, while other parts suffer from hundreds of meters of coastal retreat. Such variability is in line with probabilistic estimates of



coastal recession of natural shorelines [14] attempting to include local factors and ultimately providing coastal managers with quantitative information on the risk of retreat.

Yet, the most commonly used method to estimate coastal recession due to SLR remains the deterministic Bruun Rule [20] for its ease of application and lack of simple alternatives, despite having been a controversial tool for decades [14]. Comparing the coastal recession as observed and as predicted from the Bruun Rule for our modelled deltas, we find that the Bruun rule significantly underestimates the observed recession (Table 1), and the underestimation of coastal recession with the Bruun rule would be even larger when statically inundating the deltaic coasts. This finding reiterates the limitations of the Bruun Rule and signals the need to move to more advanced methods for reliable estimates of coastal recession to better inform coastal management.

#### 4. Discussion

Our model simulations show a limited difference between river-dominated, wave-influenced and tide-influenced deltas in their dynamic response to SLR. The physics-based numerical modelling approach is generic, with boundary conditions representative for many natural deltaic systems. Despite many morphological similarities with natural deltas (Table 1, percentage wetted in absence of SLR; Table 2, shoreline rugosity and number of channels draining into ocean), these are idealized models that lack many of the complexities generally seen in nature. For example, salinity gradients, graded sediment, engineering structures and ecological feedbacks [36] are, amongst others, not included but are likely to affect the results. For simplicity, a yearly river flood is assumed to coincide with a representative tidal cycle or a coastal storm event in our simulations. Future studies may seek to explore time-varying marine and fluvial forcing because the timing of their morphologically relevant events (e.g., river flood, spring tide, storm wave event) determines the coastal response and the long-term (100 years) delta evolution. The applied marine delta forcing in this study is relatively small (Table 1) suggesting that the simulations are most informative for river-dominated deltas with limited marine forcing.

These findings provide the first quantitative predictions for the landward translation of deltaic shorelines while allowing for a dynamic response. Such predictions of dynamic morphologic change can be included in Climate and Earth System Models while also informing local management of deltaic areas. In essence, they confirm the over-prediction of land submergence and coastal retreat by static inundation models also observed for natural coastal systems [12]. This corroborates the inadequacy of approaches employing static models to predict flooding and coastal recession potential of future deltas. Interestingly, our observations also indicate that the over-prediction of static compared to dynamic models halts between 47 cm and 82 cm SLR due to the inability of morphologic processes to dynamically keep up with higher SLR rates for the given conditions. This would imply that deltas experiencing an SLR larger than 47 cm in 100 years become, in effect, statically inundated even when dynamical response is included. With an observational SLR rate of 3.2–3.4 mm per year for the period between 1993 and 2014 [37], this threshold between dynamically-responding deltas and deltas that become statically inundated due to the inability of morphologic processes to keep up with higher SLR rates is not too far off. Compared to the observational SLR rate, the applied SLR of 26 cm over a century will require a decrease in the current rate of SLR while the SLR scenario of 82 cm over a century requires a significant increase in the current rate of SLR.

Human engineering activities are contributing to the loss of delta land and ecosystems. In addition to a rising sea level, many coastal and delta cities suffer from land subsidence mainly due to reduced sediment loads [38] and groundwater extraction [33]. In major cities like New Orleans, Jakarta and Bangkok the combined effects of SLR and land subsidence significantly increase flood vulnerability and economic costs due to severe infrastructural damage [32]. As subsidence and SLR in effect both lead to increasingly submerged deltas, the results of the modelled deltas can also be used to understand the ability of an area to dynamically respond to subsidence. With subsidence rates exceeding present-day SLR rates up to a factor of ten in some locations [32], the ability to respond

dynamically using morphological processes is likely limited and impacts are therefore expected to be significant, particularly in delta cities with fixed infrastructure.

Our results also have implications for ecosystem-based coastal defense [16] and delta restoration [4] initiatives. Delta coastal ecosystems are known to be highly dynamic environments with significant capacity to adapt to SLR due to non-linear feedbacks between the hydrodynamics, morphodynamics and ecological processes [11]. The buffer capacity that ecosystems provide in addition to the dynamic adjustment of delta morphology may well be able to overcome the loss of intertidal area as observed in this study (Figure 3), particularly in environments with suspended sediment and vegetation-enhancing sediment trapping and vertical accretion [11]. Furthermore, the initiatives in the Mississippi River delta to build new land [39] in a region with a projected SLR close to the global mean [7,8] will have to consider the dynamically adapted bed level distribution due to SLR. In the absence of ecological feedbacks and engineering structures, our simulations show an overall loss of suitable coastal habitats, particularly in the intertidal zone. Ecological processes may mitigate the impacts of SLR on the physical delta environment but the sustainability and long-term safety of such ecosystem-based coastal defenses and delta restoration initiatives can only be comprehensively explored by integrating ecosystem [11,36] and morphological dynamics in response to SLR.

## 5. Conclusions

This study provides the first quantitative comparison of dynamic and static delta response to SLR. We performed 12 morphodynamic simulations by varying the type of deltaic coastal forcing (three types) and the rate of SLR (four scenarios). The reported quantitative information on coastal flooding, shoreline retreat and ecological habitat loss improves our understanding of how twenty-first century projected sea-level rise is transferred to coastal impacts, provides input into Climate and Earth System models, and informs local coastal management. The idealized numerical model simulations show that the ability to dynamically respond to SLR is similar for river-dominated, wave-influenced and tide-influence deltas. Therefore, the potential for flooding and coastal retreat as a result of SLR is equally large for these delta types, and primarily governed by the regional differences in SLR. We find that static models overestimate the coastal impact. Sediment composition and ecological feedbacks may provide important mitigation mechanisms in shaping future deltas and will require further research for a comprehensive understanding.

**Supplementary Materials:** The following videos are available online at [www.mdpi.com/2077-1312/5/2/24/s1](http://www.mdpi.com/2077-1312/5/2/24/s1). Video S1: R\_0 (Control Run: river flow and no SLR); Video S2: R\_26 (River flow and 26 cm SLR); Video S3: R\_47 (River flow and 47 cm SLR); Video S4: R\_82 (River flow and 82 cm SLR); Video S5: RT\_0 (River flow and Tides but no SLR); Video S6: RT\_26 (River flow and Tides and 26 cm SLR); Video S7: RT\_47 (River flow and Tides and 47 cm SLR); Video S8: RT\_82 (River flow and Tides and 82 cm SLR); Video S9: RW\_0 (River flow & Waves but no SLR); Video S10: RW\_26 (River flow and Waves and 26 cm SLR); Video S11: RW\_47 (River flow and Waves and 47 cm SLR); Video S12: RW\_82 (River flow and Waves and 82 cm SLR).

**Acknowledgments:** W.L. was supported by the European Community's Horizon 2020 Programme through a grant to the budget of the Integrated Infrastructure Initiative HYDRALAB+, Contract No. 654110. A.S. received funding from the NWO Netherlands Polar Programme.

**Author Contributions:** W.L. designed and conducted the numerical modelling and analyses. W.L. and A.S. wrote the results and conclusions and prepared the manuscript.

**Conflicts of Interest:** The authors declare no conflict of interest. The founding sponsors had no role in the design of the study; in the collection, analyses, or interpretation of data; in the writing of the manuscript, and in the decision to publish the results.

## References

- Nicholls, R.J.; Wong, P.P.; Burkett, V.R.; Codignotto, J.O.; Hay, J.E.; McLean, R.F.; Ragoonaden, S.; Woodroffe, C.D. Coastal systems and low-lying areas. In *Climate Change 2007: Impacts, Adaptation and Vulnerability. Contribution of Working Group II to the Fourth Assessment Report of the Intergovernmental Panel on Climate Change*; Parry, M.L., Canziani, O.F., Palutikof, J.P., van der Linden, P.J., Hanson, C.E., Eds.; Cambridge University Press: Cambridge, UK, 2007; pp. 315–356.
- Wong, P.P.; Losada, I.J.; Gattuso, J.-P.; Hinkel, J.; Khattabi, A.; McInnes, K.; Saito, Y.; Sallenger, A. Chapter 5: Coastal Systems and Low-Lying Areas. In *Climate Change 2014: Impacts, Adaptation, and Vulnerability. Part A: Global and Sectoral Aspects. Contribution of Working Group II to the Fifth Assessment Report of the Intergovernmental Panel on Climate Change*; Field, C.B., Barros, V.R., Dokken, D.J., Mach, K.J., Mastrandrea, M.D., Bilir, T.E., Chatterjee, M., Ebi, K.L., Estrada, Y.O., Genova, R.C., et al., Eds.; Cambridge University Press: Cambridge, UK and New York, NY, USA, 2014; pp. 361–409.
- Church, J.A.; Clark, P.U.; Cazenave, A.; Gregory, J.M.; Jevrejeva, S.; Levermann, A.; Merrifield, M.A.; Milne, G.A.; Nerem, R.S.; Nunn, P.D.; et al. Sea Level Change. In *Climate Change 2013: The Physical Science Basis. Contribution of Working Group I to the Fifth Assessment Report of the Intergovernmental Panel on Climate Change*; University Press: Cambridge, UK, 2013.
- Edmonds, D.A.; Slingerland, R.L. Significant effect of sediment cohesion on delta morphology. *Nat. Geosci.* **2010**, *3*, 105–109. [[CrossRef](#)]
- Galloway, W.D. Process Framework for describing the morphologic and stratigraphic evolution of deltaic depositional systems. In *Deltas, Models for Exploration*; Broussard, M.E., Ed.; Houston Geological Society: Houston, TX, USA, 1975; pp. 86–98.
- Nienhuis, J.H.; Ashton, A.D.; Giosan, L. What makes a delta wave-dominated? *Geology* **2015**, *43*, 511–514. [[CrossRef](#)]
- Slangen, A.B.A.; Katsman, C.A.; van de Wal, R.S.W.; Vermeersen, L.L.A.; Riva, R.E.M. Towards regional projections of twenty-first century sea-level change based on IPCC SRES scenarios. *Clim. Dyn.* **2011**, *38*, 1191–1209. [[CrossRef](#)]
- Carson, M.; Köhl, A.; Stammer, D.; Slangen, A.B.A.; Katsman, C.A.; van de Wal, R.S.W.; Church, J.; White, N. Coastal sea level changes, observed and projected during the 20th and 21st century. *Clim. Change* **2016**, *134*, 269–281. [[CrossRef](#)]
- Barbier, E.B.; Hacker, S.D.; Kennedy, C.; Koch, E.W.; Stier, A.C.; Silliman, B.R. The value of estuarine and coastal ecosystem services. *Ecol. Monogr.* **2011**, *81*, 169–193. [[CrossRef](#)]
- Redfield, A.C. Development of a New England Salt Marsh. *Ecol. Monogr.* **1972**, *42*, 201–237. [[CrossRef](#)]
- Kirwan, M.L.; Guntenspergen, G.R.; D'Alpaos, A.; Morris, J.T.; Mudd, S.M.; Temmerman, S. Limits on the adaptability of coastal marshes to rising sea level. *Geophys. Res. Lett.* **2010**, *37*, L23401. [[CrossRef](#)]
- Lentz, E.E.; Thieler, E.R.; Plant, N.G.; Stippa, S.R.; Horton, R.M.; Gesch, D.B. Evaluation of dynamic coastal response to sea-level rise modifies inundation likelihood. *Nat. Clim. Chang.* **2016**, *6*, 1–6. [[CrossRef](#)]
- Strauss, B.H.; Ziemlinski, R.; Weiss, J.L.; Overpeck, J.T. Tidally adjusted estimates of topographic vulnerability to sea level rise and flooding for the contiguous United States. *Environ. Res. Lett.* **2012**, *7*, 14033. [[CrossRef](#)]
- Ranasinghe, R.; Callaghan, D.; Stive, M.J.F. Estimating coastal recession due to sea level rise: Beyond the Bruun rule. *Clim. Change* **2012**, *110*, 561–574. [[CrossRef](#)]
- Sweet, W.V.; Park, J. From the extreme to the mean: Acceleration and tipping points of coastal inundation from sea level rise. *Earth's Future* **2014**, *2*, 579–600. [[CrossRef](#)]
- Temmerman, S.; Meire, P.; Bouma, T.J.; Herman, P.M.J.; Ysebaert, T.; de Vriend, H.J. Ecosystem-based coastal defence in the face of global change. *Nature* **2013**, *504*, 79–83. [[CrossRef](#)] [[PubMed](#)]
- Lesser, G.; Roelvink, J.; van Kester, J.; Stelling, G. Development and validation of a three-dimensional morphological model. *Coast. Eng.* **2004**, *51*, 883–915. [[CrossRef](#)]
- Schuurman, F.; Kleinhans, M.G.; Marra, W.A. Physics-based modeling of large braided sand-bed rivers: Bar pattern formation, dynamics, and sensitivity. *J. Geophys. Res. Earth Surf.* **2013**, *118*, 2509–2527. [[CrossRef](#)]
- Moss, R.H.; Edmonds, J.A.; Hibbard, K.A.; Manning, M.R.; Rose, S.K.; van Vuuren, D.P.; Carter, T.R.; Emori, S.; Kainuma, M.; Kram, T.; et al. The next generation of scenarios for climate change research and assessment. *Nature* **2010**, *463*, 747–756. [[CrossRef](#)] [[PubMed](#)]

20. Bruun, P. The Bruun rule of erosion by sea-level rise: A discussion on large-scale two-and three-dimensional usages. *J. Coast. Res.* **1988**, *4*, 627–648.
21. Booij, N.; Ris, R.C.; Holthuijsen, L.H. A third-generation wave model for coastal regions, 1, Model description and validation. *J. Geophys. Res.* **1999**, *104*, C4. [[CrossRef](#)]
22. Van Rijn, L.C. Sediment transport, part I: Bed load transport. *J. Hydraul. Eng.* **1984**, *110*, 1431–1456. [[CrossRef](#)]
23. Van Rijn, L.C. Sediment transport, part II: Suspended load transport. *J. Hydraul. Eng.* **1984**, *110*, 1613–1641. [[CrossRef](#)]
24. Engelund, F.; Hansen, E. *A Monograph on Sediment Transport in Alluvial Streams*; Teknisk Forlag: Kobenhavn, Denmark, 1967.
25. Roelvink, J.A. Coastal morphodynamic evolution techniques. *Coast. Eng.* **2006**, *53*, 277–287. [[CrossRef](#)]
26. Geleynse, N.; Voller, V.R.; Paola, C.; Ganti, V. Characterization of river delta shorelines. *Geophys. Res. Lett.* **2012**, *39*, L17402. [[CrossRef](#)]
27. Wellner, R.; Beaubouef, R.; van Wagoner, J.; Roberts, H.; Sun, T. Jet-Plume Depositional Bodies—The Primary Building Blocks of Wax Lake Delta. *Gulf Coast Assoc. Geol. Soc. Trans.* **2005**, *55*, 867–909.
28. Kleinhans, M.G.; van Dijk, W.M.; van de Lageweg, W.I.; Hoyal, D.C.J.D.; Markies, H.; van Maarseveen, M.; Roosendaal, C.; van Weesep, W.; van Breemen, D.; Hoendervoogt, R.; et al. Quantifiable effectiveness of experimental scaling of river- and delta morphodynamics and stratigraphy. *Earth Sci. Rev.* **2014**, *133*, 43–61. [[CrossRef](#)]
29. Wolinsky, M.A.; Edmonds, D.A.; Martin, J.; Paola, C. Delta allometry: Growth laws for river deltas. *Geophys. Res. Lett.* **2010**, *37*, L21403. [[CrossRef](#)]
30. Jerolmack, D.J. Conceptual framework for assessing the response of delta channel networks to Holocene sea level rise. *Quat. Sci. Rev.* **2009**, *28*, 1786–1800. [[CrossRef](#)]
31. Syvitski, J.P.M.; Saito, Y. Morphodynamics of deltas under the influence of humans. *Glob. Planet. Change* **2007**, *57*, 261–282. [[CrossRef](#)]
32. Erkens, G.; Bucx, T.; Dam, R.; de Lange, G.; Lambert, J. Sinking coastal cities. *Proc. Int. Assoc. Hydrol. Sci.* **2015**, *372*, 189–198. [[CrossRef](#)]
33. Wada, Y.; van Beek, L.P.H.; van Kempen, C.M.; Reckman, J.W.T.M.; Vasak, S.; Bierkens, M.F.P. Global depletion of groundwater resources. *Geophys. Res. Lett.* **2010**, *37*. [[CrossRef](#)]
34. Kirwan, M.L.; Murray, A.B.; Boyd, W.S. Temporary vegetation disturbance as an explanation for permanent loss of tidal wetlands. *Geophys. Res. Lett.* **2008**, *35*, L05403. [[CrossRef](#)]
35. Kirwan, M.L.; Murray, A.B. A coupled geomorphic and ecological model of tidal marsh evolution. *Proc. Natl. Acad. Sci. USA* **2007**, *104*, 6118–6122. [[CrossRef](#)] [[PubMed](#)]
36. Temmerman, S.; Kirwan, M.L. Building land with a rising sea. *Science* **2015**, *349*, 588–589. [[CrossRef](#)] [[PubMed](#)]
37. Ablain, M.; Legeais, J.F.; Prandi, P.; Marcos, M.; Fenoglio-Marc, L.; Dieng, H.B.; Benveniste, J.; Cazenave, A. Satellite Altimetry-Based Sea Level at Global and Regional Scales. *Surv. Geophys.* **2017**, *38*, 7–31. [[CrossRef](#)]
38. Syvitski, J.P.M.; Kettner, A.J.; Overeem, I.; Hutton, E.W.H.; Hannon, M.T.; Brakenridge, G.R.; Day, J.; Vörösmarty, C.; Saito, Y.; Giosan, L.; et al. Sinking deltas due to human activities. *Nat. Geosci.* **2009**, *2*, 681–686. [[CrossRef](#)]
39. Kim, W.; Mohrig, D.; Twilley, R.; Paola, C.; Parker, G. Is It Feasible to Build New Land in the Mississippi River Delta? *EOS Trans. Am. Geophys. Union* **2009**, *90*, 373–374. [[CrossRef](#)]

